ICSTI
6th International Congress on the Science and Technology of Ironmaking - ICSTI
42th Ironmaking and Raw Materials Seminar/ 42º Seminário de Redução de Minério de Ferro e Matérias-primas
13th Brazilian Symposium on Iron Ore/ 13º Seminário Brasileiro de Minério de Ferro
ISSN 2176-3135

ANALYSIS OF PCDD AND PCDF EMISSIONS ON THE IRON ORE SINTERING PROCESS BASED ON ALTERNATIVE GASEOUS FUELS FROM STEELWORKS[1]

Jose Adilson de Castro[2]
Vagner Silva Guilherme[2]
Alexandre Bôscaro França[2]
Yasushi Sazak[3]
Jun-ichiro Yagi[4]

Abstract

Recently the technology of gas utilization on the iron ore sintering process has been proposed as alternative for reducing the environmental impact and improvements on the sinter quality with lower return(<5mm). This paper deals with the numerical simulation of this new technology in order to evaluate the emissions of poly chlorinated di-benzene dioxin (PCDD) and Poly Chlorinated di-benzene furan (PCDF). The proposed methodology is to partially replace the solid fuel(coke breeze) by steelworks gases such as coke oven gas (COG), blast furnace gas (BFG) and synthetic gas obtained by mixture of these gases. A multiphase mathematical model based on transport equations of momentum, energy and chemical species coupled with chemical reaction rates and phase transformations is proposed to analyze the inner process parameters and the rates of PCDD and PCDF formation. A base case representing the actual industrial operation of a large sintering machine is used with thermocouples inserted into the sintering bed to record the inner bed temperatures and compare with model predictions in order to obtain model validation and parameters adjustment. Good agreement of the temperature pattern was obtained for the base case and thus, the model was used to predict four cases of fuel gas utilization: a) 4% of the wind boxes inflow from N01-N12 wind boxes COG, b) same condition with BFG, c) same condition with 50% COG and 50% BFG and d) mixture of 25% COG and 75% BFG. The model predictions indicated that for all cases, except only BFG, the sintering zone is enlarged and the solid fuel consumption is decreased. In order to maximize the steelworks gas utilization it is recommended the use of mixture of COG and BFG with optimum inner temperature distribution. For all cases of gas utilization the PCDD and PCDF emissions decreased.

Keywords: Sintering; Modeling; Fuels; Multiphase flow.

[1] *Technical contribution to the 6th International Congresso on the Sicence and Technology of Ironmaking – ICSTI,42nd International Meeting on Ironmaking and 13th International Symposium on Iron Ore, October14th to18th,2012, Rio de Janeiro, RJ, Brazil.*

[2] *Graduate Program on Metallurgical Engineering and Mechanical Engineering-Federal Fluminense University - Volta Redonda, RJ, Brazil, 27255-125 Tel: +55 24-2107-3756*

[3] *Environmental Laboratory Graduate Institute of Ferrous Technology-POSTECH-Pohang University of Science and Technology, San 31 Hyojay-Dong, Nam-Gu, Pohang, 790-784, South Korea*

[4] *Emeritus Professor at Tohoku University, Sendai, Japan*

ISSN 2176-3135

1INTRODUCTION

The sintering process in the integrated steelworks is responsible to provide high quality of raw materials for the blast furnace. The process is complex and involves various physical and chemical phenomena such as heat, mass and momentum transfer coupled with chemical reactions.[1-4] These phenomena take place simultaneously increasing considerably the complexity of process analysis. The raw materials used in the iron ore sintering process are obtained from several sources, like iron ore(mining sinter feed), dust recycling within the steelworks and addition of slag agents for blast furnace and enhance the sinter product quality, namely reactivity and mechanical strength, which plays crucial role on the blast furnace performance and reducing agent consumption. In the conventional operation, the combustion of the solid fuels(coke breeze or anthracite) begins at the top layers, and as it moves, a relative narrow band of ignition zone moves downward through the bed, that can be strongly affected by the quality of the raw materials.[5-9] Several chemical reactions and phase transformations are affected not only by the heat front modifications but also due to changes in local gas composition and initial melting temperature of the mixture of raw materials. When local temperature and composition of the solid is reached, mostly the phase transformations are driven by heat supply and diffusion that take place within the sinter bed with the mechanism of liquid formation playing the major role. The materials partially melt down when the local temperature reaches the melting temperature and as it moves, the contact with cold gas promotes the re-solidification and thus, the particle agglomeration forms a continuous and porous sinter cake. The final sinter cake properties are strongly dependent upon the thermal cycle, initial raw material composition and thermophysical properties. In this paper, the sintering process is analyzed, when fuel gases such as natural gas (NG), coke oven gas(COG) and blast furnace gas(BFG) is sucked through the sinter bed. It is expected that the fuel gas reaching the thermal front combust earlier leading to the result of enlargement of the sintering zone, as shown in Fig. 1, which in turn, can increase the liquid formed(mushy) and residence time of the materials within the sintering temperature improving the amount of calcium ferrite and bonding phases. Several attempts have been made aiming at predicting the final properties of the sinter product. One of the most important parameter is the size distribution which influences strongly the sinter performance within the blast furnace. Previous models addressed the sintering phenomena[2-5] and mathematical models to predict the final size distribution of the sinter,[6] however, these models did not considered detailed kinetics of the sintering phenomena, which strongly affect the final size distribution.[6,7]. Kasai et al.[7] investigated the influence of sinter structure on the macroscopic sinter properties. A detailed explanation of the sintering mechanism and particle interaction was provided in order to clarify the bonding forces responsible for the sinter structure and strength. In the present days, the reduction of CO_2 emissions has become an urgent issue in the steel industry as countermeasure for greenhouse emissions.[1] It is estimated that nearly 60% of the steel industry emissions are attributed to the pig iron production unit operations, which includes sintering and blast furnace processes, and only the sintering process represents around 20% of this amount.[1,5] Therefore, sintering and blast furnace processes offer good opportunities to decrease the CO_2 emissions since mall decrease in coke breeze consumption and bonding agent used in iron ore sintering process could decisively contribute to decrease the environmental load of the steelmaking industry. Therefore, alternative sources of energy with lower

ISSN 2176-3135

environmental impact or replacement of the coke breeze by in-house gaseous fuel are attractive technologies to enhance the iron ore sintering process.

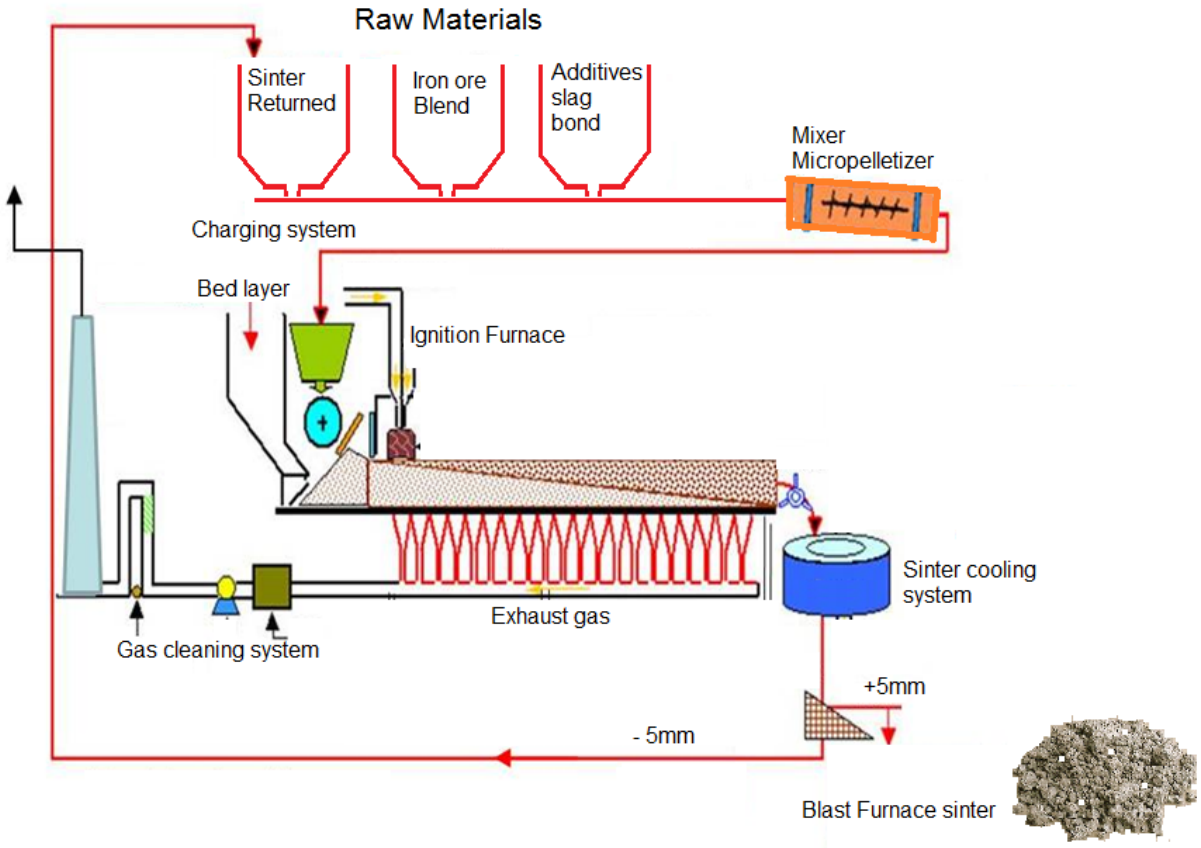

Figure 1.Schematic view of the sintering process facilities.

The concept of gaseous injection into the sinter bed has been successfully applied and enhancement of the sinter properties related to reducibility and strength have been observed[1], in addition to drastically decrease the return sinter(<5mm). In this perspective, the present work aims to apply a comprehensive multiphase multicomponent mathematical model to analyze the effect of gaseous fuels such as natural gas, coke oven and blast furnace gases through the sinter bed of an industrial sintering machine and quantify the impact of this technology on the sintering process of iron ore with regard to the PCDD and PCDF emissions[5,9,10].

2METHODOLOGY

2.1 Model Concept

A model to evaluate the coupled phenomena of PCDD and PCDF formation in the sintering process of an industrial strand machine is proposed based on a multiphase, multi-component transport equations of mass, momentum and energy for gas, solid and liquid phases taking into account the local phenomena of porous sinter formation, as schematically shown in Fig. 2. This model considers the initial quasi-particle already formed and as the reactions take place, multiphase phenomena occur. Therefore a model based on multiphase transport phenomena is expected to be suitable for modeling the mass, momentum and energy transfer in the sinter bed. The chemical species are individually taken into account by solving the transport

ISSN 2176-3135

equation of each chemical species of the gas and solid phases. The solid phase includes the mixture of iron ore sinter feed, fine sinter(returned fine sinter), coke breeze(or other solid fuel), scales(fines from steel plant), fluxes and limestone. The liquid phase is composed of melted and formed components in the liquid phase.[2-9] The re-solidified phase comprises the liquids re-solidified and phases formed during the re-solidification process.

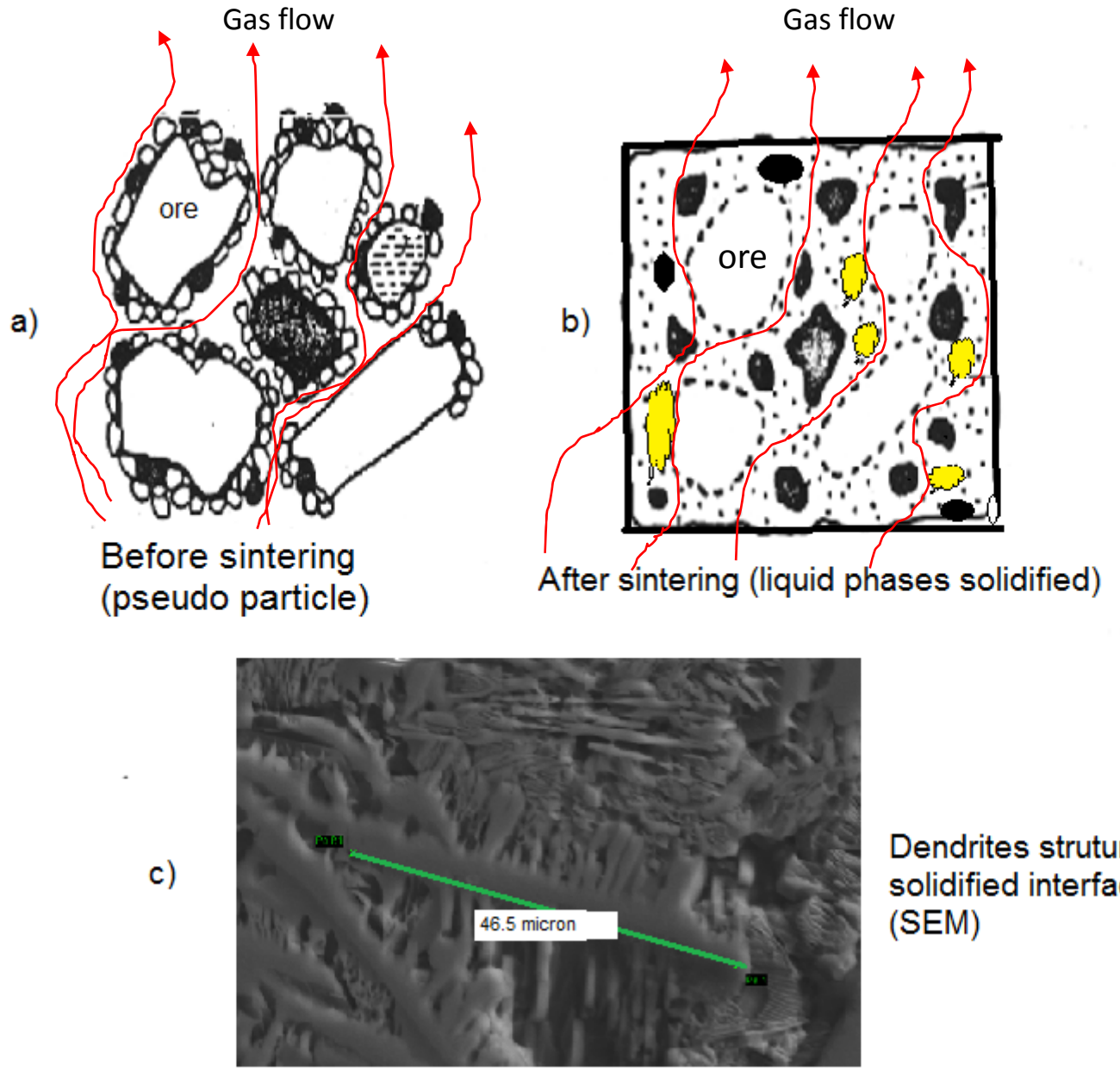

Figure 2 Transport phenomena and liquid phase formation in an elemental volume of the sinter bed.

Momentum:

$$\frac{\partial\left(\rho_i \varepsilon_i u_{i,j}\right)}{\partial t} + \frac{\partial\left(\rho_i \varepsilon_i u_{i,k} u_{i,j}\right)}{\partial x_k} = \frac{\partial}{\partial x_k}\left(\mu_i \frac{\partial u_{i,j}}{\partial x_k}\right) - \frac{\partial P_i}{\partial x_j} - F_j^{i-l} \quad (1)$$

Continuity:

ISSN 2176-3135

$$\frac{\partial(\rho_i \varepsilon_i)}{\partial t} + \frac{\partial(\rho_i \varepsilon_i u_{i,k})}{\partial x_k} = \sum_{m=1}^{Nreacts} M_n r_m \quad (2)$$

Enthalpy balance:

$$\frac{\partial(\rho_i \varepsilon_i H_i)}{\partial t} + \frac{\partial(\rho_i \varepsilon_i u_{i,k} H_i)}{\partial x_k} = \frac{\partial}{\partial x_k}\left(\frac{k_i}{C_{p_i}} \frac{\partial H_i}{\partial x_k}\right) + E^{i-l} + \sum_{m=1}^{Nreacts} \Delta H_m r_m \quad (3)$$

The chemical species are individually considered within the phase, for gas, or components of the solid or liquid phases, as presented in equation (4).

$$\frac{\partial(\rho_i \varepsilon_i \phi_n)}{\partial t} + \frac{\partial(\rho_i \varepsilon_i u_{i,k} \phi_n)}{\partial x_k} = \frac{\partial}{\partial x_k}\left(D_n^{eff} \frac{\partial \phi_n}{\partial x_k}\right) + \sum_{m=1}^{Nreacts} M_n r_m \quad (4)$$

Where indexes ***i*** and ***l*** represent the phases, ***j*** and ***k*** are the indexes for coordinates component direction ***n*** is chemical species and ***m*** the indicator of the reactions, M is the molecular weight of the species, ***P*** is phase pressure, ***F*** is component of momentum interactions among the phases and ***r*** is the rate of chemical reactions. ρ,ε,Cp, k and ΔH are phase density, volume fractions, heat capacity, heat conductivity and heat due to chemical reactions, respectively. The quantity E^{i-l} is the heat transfer among the phases and accounts for convective and radiation heat transfer, since conductive heat transfer is include in eq. 3. The gas -solids momentum interactions are represented by F^{i-l}. The model equations are completed with suitable correlations for the thermophysical properties of the phases, rate equations for the source terms and the initial and boundary conditions representing the sintering process. The chemical species considered in this model are presented in Table 1.

2.2 Source Terms

The momentum transfer between the solid and gas are modeled based on the modified Ergun's equation, which takes into account the local soft-melting behavior of the raw materials with the volume fraction and effective diameters modified by the soft-melting data, as follows[2-10]

$$F_g^s = \left[1.75\,\rho_g + \frac{150\,\mu_g}{\left|\vec{U}_g - \vec{U}_s\right|}\left(\frac{\varepsilon_s}{d_s \varphi_s}\right)\right]\left(\frac{\varepsilon_s}{(1-\varepsilon_s)^3 d_s \varphi_s}\right)\left|\vec{U}_g - \vec{U}_s\right|\left(u_{g,j} - u_{s,j}\right) \quad (5)$$

The overall heat transfer coefficient between the gas and the packed bed[11-15]is given by equation (6).

$$E^{g-s} = \frac{6\varepsilon_s}{d_s \varphi_s}\frac{k_g}{(d_s \varphi_s)}\left[2 + 0.39\left(\mathrm{Re}_{g-s}\right)^{1/2}\left(\mathrm{Pr}_g\right)^{1/3}\right]\left(T_g - T_s\right) \quad (6)$$

As shown in eq. 6, the gas-solid interface heat transfer is given by the product of the overall effective heat transfer coefficient, the interfacial area and the average temperature differences of the bed and gas phase. The parameters of the sinter bed ε_s d_s and φ_s are temperature dependent and account for the effective volume fraction, particle diameter and shape factor, respectively, which strongly affect the momentum and energy transfer on the soft-melting zone. The solid diameters and shape factors are given as raw materials properties from the harmonic average of the particle size distributions. In the present model these parameters are calculated by using soft-

ISSN 2176-3135

melting experimental data for the raw materials used[2,16-20], as presented by equations (7)-(9).

$$\varepsilon_i = 1 - \left(0.403\left[100 d_i\right]^{0.14}\right)\left(1 - MAX\left(0,\ MIN\left(1,\ \left(\frac{T_s - T_{im}}{\Delta T_m}\right)\right)\right)\frac{S_m}{100}\right) \quad (7)$$

$$\varepsilon_s = \sum \varepsilon_i + \varepsilon_l + \varepsilon_{ls} \quad (8)$$

$$d_s = d_{initial} + \left(d_{final} - d_{initial}\right)\left(\frac{\varepsilon_l + \varepsilon_{ls}}{\varepsilon_s}\right)^3 \quad (9)$$

Where *i*stands for iron ore sinter feed, retuned sinter, solid fuels, fluxes and mill scales on the sintering mixture charged on the sinter bed, *l* and *ls* are the liquid and solid bridges volume fractions formed during sintering phenomena. The average size of the sintering structure are given by equation (9) with the parameters $d_{initial}$ and d_{final} representing the average particle size of the quasi particles charged in the bed and the particle size for complete sintering product[2]. In the present model these parameters are given for each sintering mixture with their own softening-melting data, where the model uses the parameters T_{im}, ΔT_m and S_m representing the initial melting temperature, meting temperature interval and percentage of shrinkage. This parameters are obtained from the pressure *vs* temperature curve obtained from the softening-melting experiment.[16-21]

2.3 Boundary and Initial Conditions

The model formulation represented by equations (1)-(4) is completed with the initial and boundary conditions. The computational domain is defined by the region of the sinter strand for the industrial scale process simulation and the equations are solved considering steady state conditions, therefore the first terms on the left of the equations are set to zero and the initial conditions are regarded as guess values for the numerical iterations. Regarding the boundary conditions for the solid phase, composition, initial and inlet particle diameters, charging particle and volume fraction distribution and moisture content are specified at the charging position of the strand. The outlet boundary condition for the solid phase is assumed to be fully developed flow and no slip condition is assumed at the sinter strand. The other boundaries such as lateral and bed surface are assumed zero velocity gradient. For the energy balance equations convective and radiation coefficients are assumed for each of these surfaces. The gas inlet and outlet flow rates are determined by the pressure drop specified for each wind box and it is calculated iteratively by considering simultaneously the momentum balance and pressure drop of each wind box. The gas inlet temperature is specified at the surface of the bed and the outlet temperature are calculate by assuming fully developed flow. As for the chemical species for the gas phase, specified values on the surface of the sinter bed are assumed and similarly the solid phase at the outlet are calculated by using fully developed flow conditions at the bottom of the bed.

2.4 Numerical Details

The multiphase model is composed of a set of partial differential equations that can only be solved by numerical method due to their nonlinearities on the boundary

ISSN 2176-3135

conditions and source terms. In this work, the set of differential equations described above is discretised by using the finite volume method and the resulting set of algebraic equations are solved by the iterative procedure using the line by line method combined with the tri-diagonal matrix solver algorithm.[21] In this paper, the numerical grid used to simulate the industrial strand of the sinter machine was discretised based on the Cartesian coordinate system with 10x140x12 = 16800 control volumes, assumed suitable for the calculations after continuous grid refinement to assure solutions independent of the control volume size. The numerical convergence was accepted for tolerance of the order of 10^{-6} for the velocity and temperature fields, meanwhile, for the chemical species the overall mass balance was accepted less than 1% for all chemical species calculated.

Table 1. Phases and chemical species considered in the model of the sintering process

		Equations of the gas phase	
Gas	Momentum		
	Energy		
	Chemical Species	N_2, O_2, CO,CO_2, H_2O, H_2, SiO, SO_2, CH_4, C_2H_6, C_3H_8, C_4H_{10}	
		Equations of the solid phase	
Solid	Momentum		
	Energy		
	Chemical Species	Coke breeze	C,Volatiles, H_2O, Al_2O_3, SiO_2, MnO, MgO, CaO, FeS, P_2O_5, K_2O, Na_2O, S_2
		Iron ore (sinter feed)	Fe_2O_3, Fe_3O_4, FeO, Fe, H_2O, Al_2O_3, SiO_2, MnO, MgO, CaO, FeS, P_2O_5, K_2O, Na_2O
		Return Sinter (bed)	Fe_2O_3, Fe_3O_4, FeO, Fe, H_2O, Al_2O_3, SiO_2, MnO, MgO, CaO, FeS, P_2O_5, K_2O, Na_2O
		Solidified materials	Fe_2O_3, Fe_3O_4, FeO, Fe, H_2O, Al_2O_3, SiO_2, MnO, MgO, CaO, FeS, P_2O_5, K_2O, Na_2O, $Ca_2Fe_3O_5$, Al_2MgO_4
		Fluxing agent	CaO, H_2O, Al_2O_3, SiO_2, MnO, MgO, TiO_2
		Sinter cake	Fe_2O_3, Fe_3O_4, FeO, Fe, H_2O, Al_2O_3, SiO_2, MnO, MgO, CaO, FeS, P_2O_5, K_2O, Na_2O, $Ca_2Fe_3O_5$, Al_2MgO_4
Liquid	Chemical Species	Intrabed liquid	Fe_2O_3, Fe_3O_4, FeO, Fe, H_2O, Al_2O_3, SiO_2, MnO, MgO, CaO, FeS, P_2O_5, K_2O, Na_2O, $Ca_2Fe_3O_5$, Al_2MgO_4

3RESULTS AND DISCUSSIONS

In order to analyze the effect of the partial substitution of the solid fuel by gaseous fuel on the PCDD and PCDF emissions in the sintering process, four cases were simulated. A base case which correspond to an actual sinter plant operation is used to demonstrate the model accuracy and thus compare with the new technology

ISSN 2176-3135

proposed based on partial substitution of the coke breeze by gaseous fuel available at the steelworks. The model validation was carried out by monitoring the sinter bed temperature into 3 distinct height of the bed by inserting encapsulated thermocouples and recording the temperature measurements along the moving bed. The data used in these calculations were the averaged values of 1h of uninterrupted operation. In this interval 3 measurement runs were obtained and the averaged values of the temperatures were used to compare with the numerical predictions. Fig. 3 presents the comparison of temperature predictions by the model and measured data obtained in the industrial sintering machine for the actual operation conditions. The calculated results were compared with the measured data obtained by thermocouples inserted within the sinter bed in fixed positions of 75 mm, 355 mm and 725 mm from top of the bed and the temperatures were recorded at intervals of 10m along the strand.

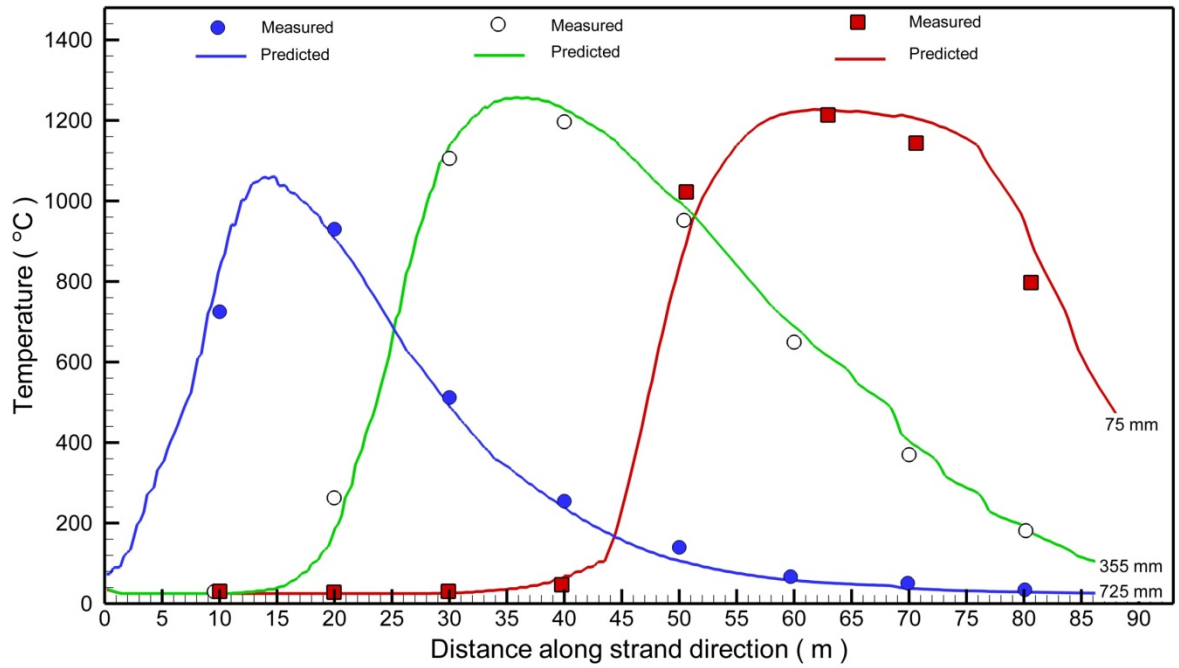

Figure 3 Temperature measured and calculated by the mathematical model

As can be observed, the measured and predicted values are in good agreement and considering that the temperature has strong correlation with all the phenomena simultaneously taking place in the sinter bed such as interface heat transfer, momentum and chemical reactions these results guarantee that the model is accurate enough to represent the industrial process of iron ore sintering. Thus, the model was used to predict new operation technologies of gaseous fuel injection. The cases analyzed in this study consider injections from the positions of the wind boxes N01 until N15 of a total of 23 wind boxes. These positions were selected to guarantee the gaseous fuel to be consumed in the bed. Four fuel injection scenarios were selected: a) 2% fuel gas through the wind boxes from N01 - N15 where replaced by dry blast furnace gas (BFG); b) same condition with natural gas (NG); c) same condition with coke oven gas(COG) and d) a mixture of 50% of COG and BFG.Figure 6 shows the comparison for the temperature pattern within the sinter bed for a vertical slice located at middle position of the bed width of the four scenarios considered. Figure 4 shows the comparative temperature pattern for the cases simulated. As can be observed, the sintering zone are gradually enlarged for BFG, NG and COG injection scenarios. This expected behavior can be explained due to

ISSN 2176-3135

the amount of heat released when the gaseous fuel is burned out.The results indicated that the sintering zone is gradually enlarged from BFG to COG gaseous fuel when compared with the base case of actual operation. The results indicated that the coke oven gas was the most effective fuel to enlarge the sintering zone while the blast furnace gas showed lower effect. Thus a combined scenario of blast furnace gas and coke oven gas is proposed to utilize both the abundant steelmaking gases. The combined scenario of BFG-COG show intermediate temperature pattern, as expected, and indicated feasible operation practice since the temperature distributions are compatible with actual operation practice.

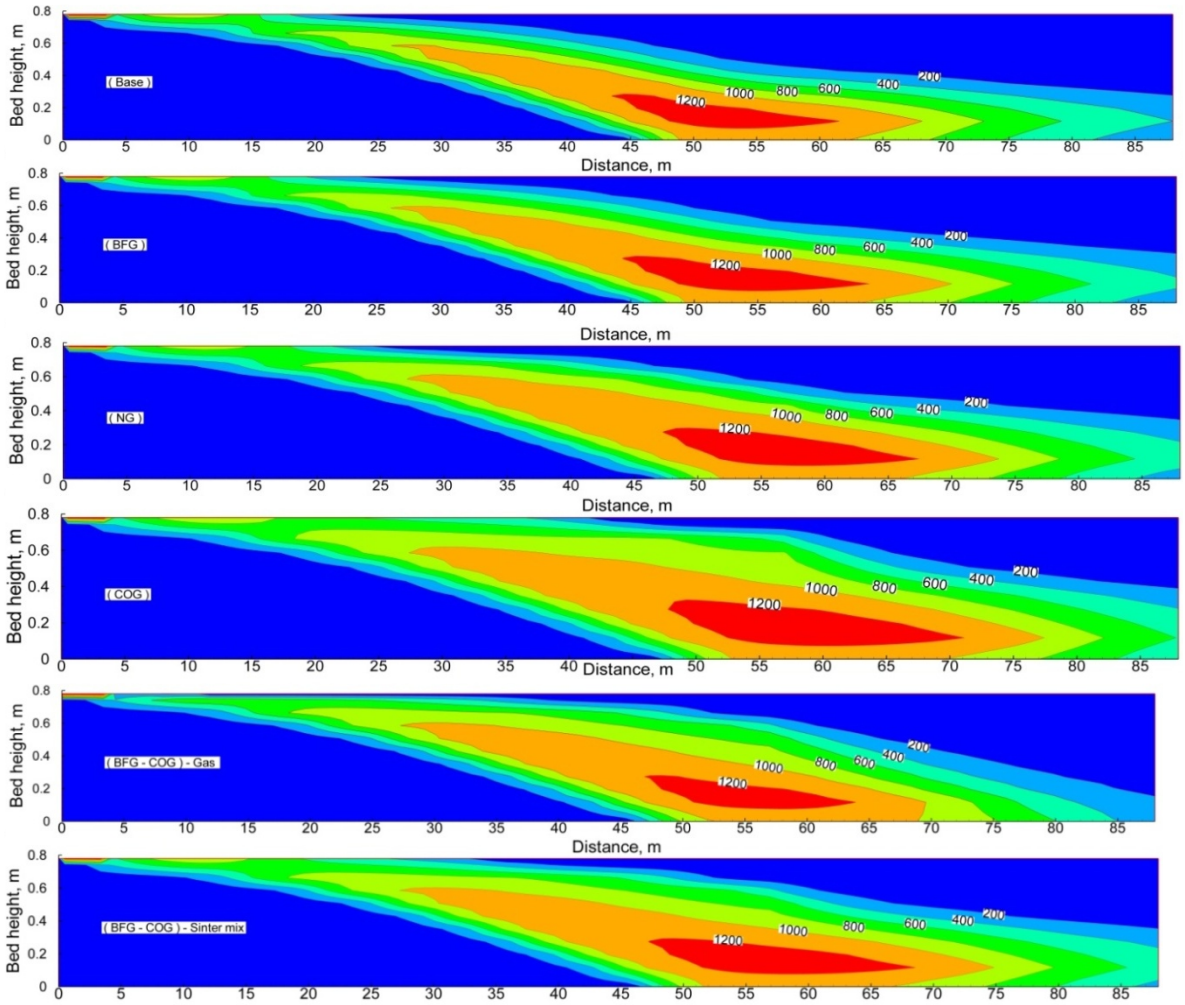

Figure 4 Comparative temperature distributions within the sinter bed

ISSN 2176-3135

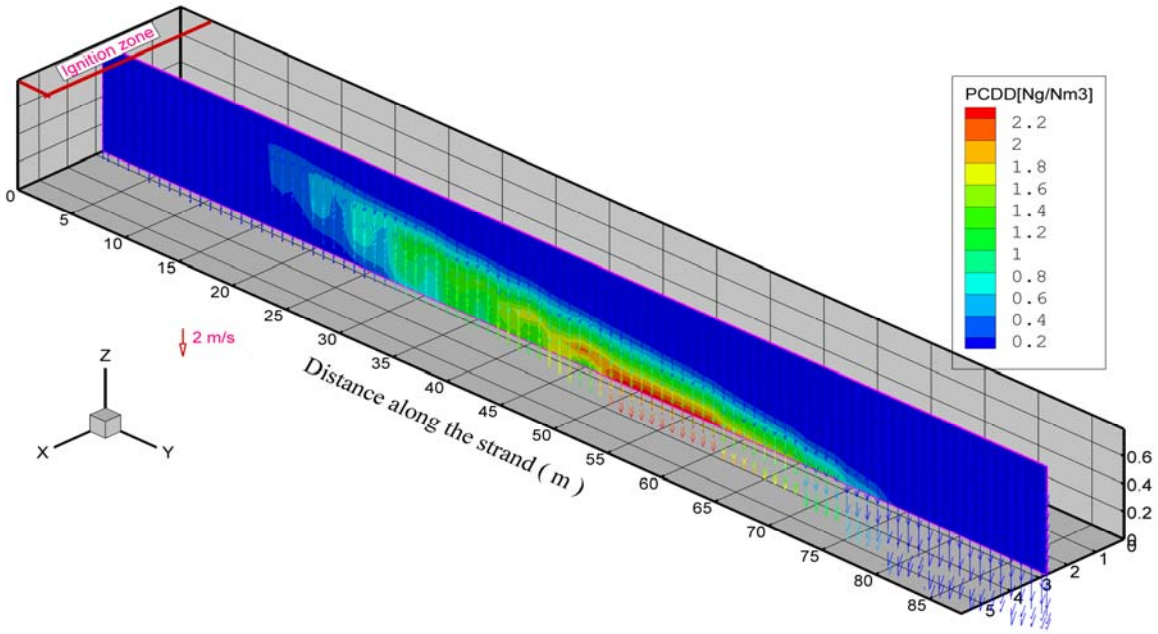

Figure 5 PCDD predictions for the base case

Figure 5 and 6 present the dioxin(PCDD) distribution pattern within the sinter bed for the base case and the combined injection of blast furnace and coke oven gases (BFG-COG). The calculated results clearly shows that when gas fuel injection is considered the net amount of dioxin generated within the bed is decreased. The reason for such a behavior can be attributed due to larger high temperature zone in the bed which contribute to destroy part of the dioxin generated in the upper part of the bed.

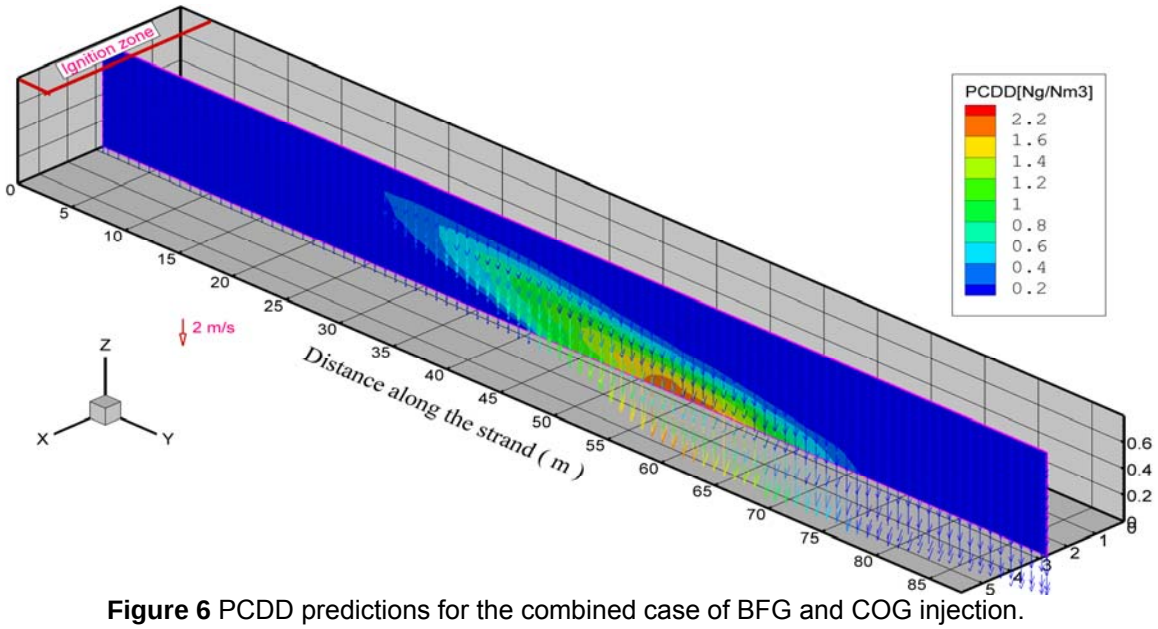

Figure 6 PCDD predictions for the combined case of BFG and COG injection.

ISSN 2176-3135

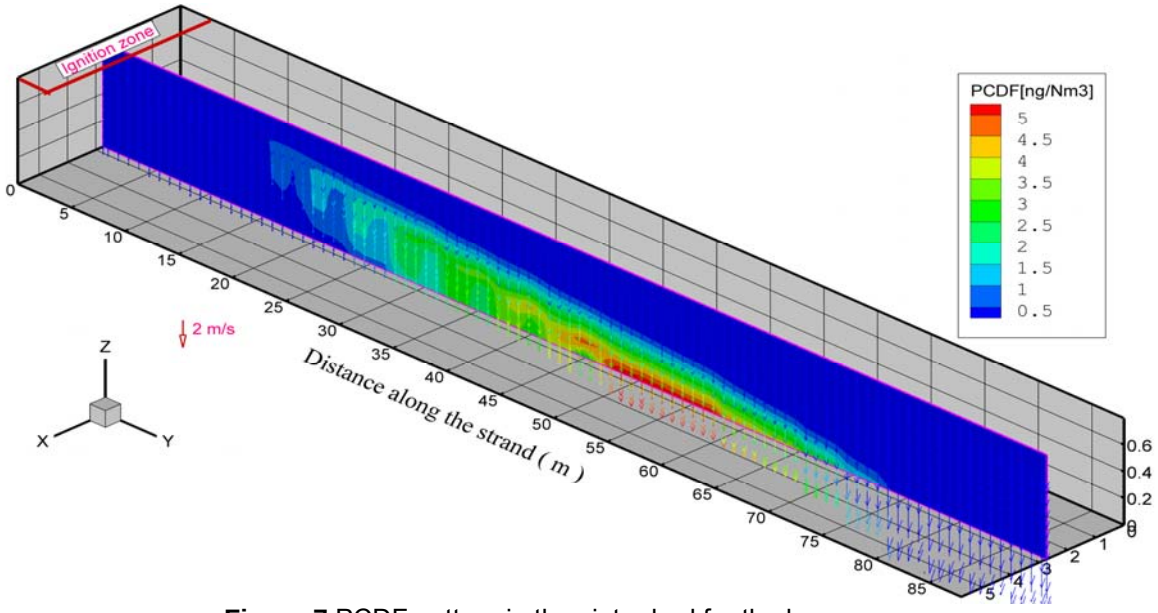

Figure 7 PCDF pattern in the sinter bed for the base case

Similar behavior can be observed for the furans net formation with higher values and location concentrated just below the BTP on the sinter bed. These patterns were expected and confirmed measurements on industrial machines carried out by Kasama, Yamamura and Watanabe.[10] Although only the base case and the BFG-COG operational practice were shown, the other injection cases showed similar pattern and as a general trend, as the sintering zone is enlarged proportionally both PCDD and PCDF decreased. Thus the calculated results indicated that, lower emissions is expected with COG injection, following NG and BFG, with the combined BFG-COG locating at intermediate value of BFG and COG. Therefore, these results confirmed that the temperature pattern within the sinter bed plays the main role on the rate of dioxins and furans net generation.

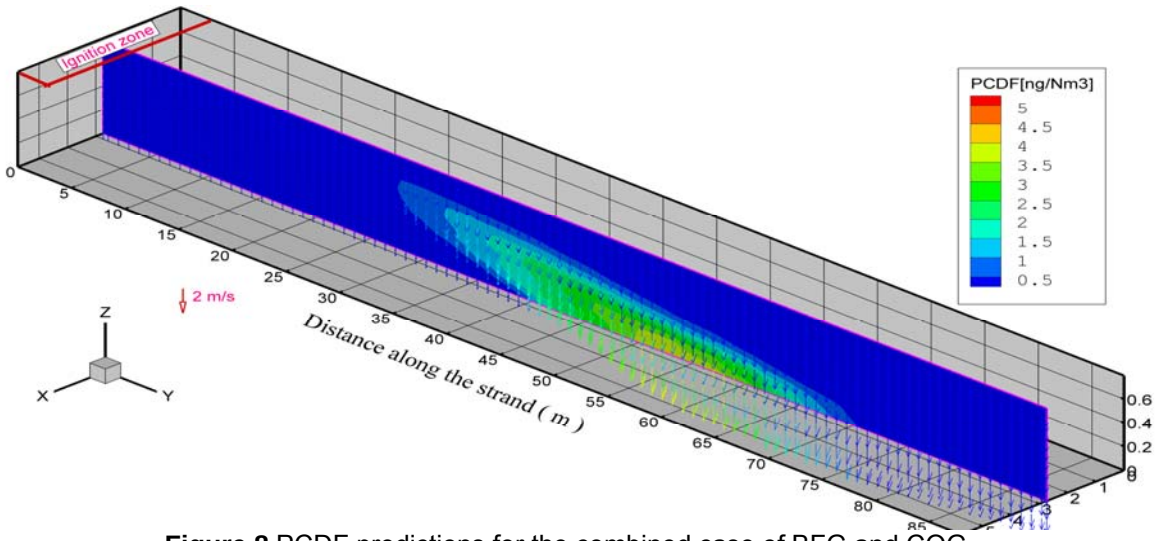

Figure 8 PCDF predictions for the combined case of BFG and COG

CONCLUSIONS

In this study new technology of gaseous fuel injection in the iron ore sinter bed is analyzed based on a multiphase mathematical model able to simulate the process

ISSN 2176-3135

phenomena in the sinter bed taking into account the coupled phenomena to analyze the possible emissions of PCDD and PCDF on the gas flue. The model is based on transport equations of momentum, energy and chemical species coupled with chemical reaction rates, which takes into account the phase flows, heat exchange and mass transfer accounting for chemical reactions and phase transformations. The model was validated by sinter bed temperature measurements obtained by inserting thermocouples into the sinter bed of the industrial sinter machine. The model was used to analyze cases of gaseous injection in the sinter bed and partially replace the solid fuel. Simulation results indicated that gaseous injection enlarges the sintering zone and enhance the sintering phenomena, confirming the same trend observed by Oyama and co-workers[1]. The calculated results indicated that solid fuel can be decreased for the gaseous fuel cases(2.4 kg for BFG, 5.9 kg for NG, 7.1 kg for COG and 6 kg for COG-BFG per ton of sinter product). The total amount o liquid phase formation increased and calcium ferrite also slightly increased. This study confirmed that this technology is attractive for steel plants which have excess of process gas such as COG and BFG and can represent considerable decrease in the solid fuel used for the sintering process and can contribute to make this process more environmentally cleaner. In this study, the calculated results confirmed that gaseous injections can contribute to reduce the PCDD and PCDF emissions and clarify that when the sintering zone is enlarged the dioxin(PCDD) and furans(PCDF) are decomposed within and the adsorption on the sintering bed decreased.

Acknowledgements

Thisstudywaspartiallysupportedby CNPq - Conselho Nacional de Desenvolvimento Científico e Tecnológico and Faperj - Fundação Carlos Chagas Filho de Amparo a Pesquisa do Estado do Rio de Janeiro - Brazil.

REFERENCES

1 N. Oyama, Y. Iwami, T. Yamamoto, S. Machida, T. Yguchi, H. Sato, K. Takeda, Y. Watanabe, and M. Shimizu: *ISIJ International*, 2011, 51, 913- 921.
2 H. Yamaoka, and T. Kawaguchi: *ISIJ International*, 2005, 45, 522- 531.
3 M.J. Cumming,. and J. A.Thurlby: *Ironmaking and Steelmaking*, 1990, 17, 245-254.
4 N. K. Nath, A.J Silva and N. Chakraborti: *Steel Research* , 1997, 68, 285-292.
5 J. , Mitterlehner, Loeffler, G., Winter, F. Hofbauer, H., Smid, H., Zwittag, E. , Buergler, T.H., Palmer, O. and Stiasni, H: ISIJ International, 2004, 44, 11-20
6 A.G., Waters, J.D. Lister, and S.K., Nicol, *ISIJ International*, 1989, 29, 274-283.
7 E Kasai, S. Komarov, K. Nushiro and M. Nakano.: *ISIJ International* , 2005, 45, 538-543.
8 J.W. Jeon, S.M. Jumg and Y. Sasaki : *ISIJ International* , 2010, 50, 1064-1070.
9 J. A. Castro, A.J. Silva, H. Nogami and J. Yagi: *TMM-Tecnologia em Metalurgia e Materiais* , 2005, 2, 45-49.
10 S. Kasama, Y. Yamamura and K. Watanabe: *ISIJ International* , 2006, 46, 1014-1019.
11 Y. Omori: 'The blast furnace phenomena and modeling', 1st edn., 631; 1987, London, Elsevier Applied Science.
12 P.R. Austin, H. Nogami, and J. Yagi: ISIJ International, 1997, 37, 748-755.
13 J. A. Castro, H. Nogami, and J. Yagi: ISIJ International, 2002, 42, 44-52.
14 P. Hou, S. Choi, W. Yang, E. Choi and H. Kang: *Materials Science and Applications*, 2011, 2, 370-380.
15 P.F. Nogueira, A.A. Castro, H. P. Pimenta: *Proceedings of the 4th International Congress on the Science and Technology of Ironmaking*, 2006, Osaka, v. 1, 671-674.

ISSN 2176-3135

16 B. Nandy, S. Chandra, D. Bhattacharjee, D. Ghosh: *Ironmaking and Steelmaking*, 2006, 33, 111-119
17 P. F. Nogueira, R. J Fruehan: *Metallurgical and Materials Transactions B*, 2006, 37B, 551-558.
18 Barnaba, P.: *Ironmaking and Steelmaking*, 1985, 12, 53-63
19 X.Lv, C. Bai,Q. Deng, X. Huang and G. Qiu : *ISIJ International* , 2011, 51, 722-727.
20 N. Oyama, T. Higuchi, S. Machida, H. Sato and K. Takeda: *ISIJ International* , 2009, 49, 650-658.
21 M.C. Melaen: *Numerical Heat Transfer, B*, 1992, 21, 1-19.